



Correction of Prompt Gamma Distribution for Improving Accuracy of Beam Range Determination in Inhomogeneous Phantom

Jong Hoon Park*, Sung Hun Kim*, Youngmo Ku*, Hyun Su Lee*, Young-su Kim*, Chan Hyeong Kim*, Dong Ho Shin[†], Se Byeong Lee[‡], Jong Hwi Jeong[‡]

*Department of Nuclear Engineering, Hanyang University, Seoul, [†]IT Convergence Technology Research Laboratory, Electronics and Telecommunications Research Institute, Daejeon, [‡]Proton Therapy Center, National Cancer Center, Goyang, Korea

Received 10 October 2017

Revised 19 December 2017

Accepted 20 December 2017

Corresponding author

Chan Hyeong Kim
(chkim@hanyang.ac.kr)
Tel: 82-2-2220-0513
Fax: 82-2-2220-4054

For effective patient treatment in proton therapy, it is therefore important to accurately measure the beam range. For measuring beam range, various researchers determine the beam range by measuring the prompt gammas generated during nuclear reactions of protons with materials. However, the accuracy of the beam range determination can be lowered in heterogeneous phantoms, because of the differences with respect to the prompt gamma production depending on the properties of the material. In this research, to improve the beam range determination in a heterogeneous phantom, we derived a formula to correct the prompt-gamma distribution using the ratio of the prompt gamma production, stopping power, and density obtained for each material. Then, the prompt-gamma distributions were acquired by a multi-slit prompt-gamma camera on various kinds of heterogeneous phantoms using a Geant4 Monte Carlo simulation, and the deduced formula was applied to the prompt-gamma distributions. For the case involving the phantom having bone-equivalent material in the soft tissue-equivalent material, it was confirmed that compared to the actual range, the determined ranges were relatively accurate both before and after correction. In the case of a phantom having the lung-equivalent material in the soft tissue-equivalent material, although the maximum error before correction was 18.7 mm, the difference was very large. However, when the correction method was applied, the accuracy was significantly improved by a maximum error of 4.1 mm. Moreover, for a phantom that was constructed based on CT data, after applying the calibration method, the beam range could be generally determined within an error of 2.5 mm. Simulation results confirmed the potential to determine the beam range with high accuracy in heterogeneous phantoms by applying the proposed correction method. In future, these methods will be verified by performing experiments using a therapeutic proton beam.

Keywords: Proton therapy, Beam range, Prompt gamma, Heterogeneous phantom, Multi-slit prompt-gamma camera

Introduction

Currently, there is an increased number of proton-treatment facilities that use proton beams to treat tumors, and there is also an increased number of patients requiring such treatment. Depending on the physical properties of

the Bragg peak, a proton beam can deliver a concentrated dose to a tumor. This property minimizes the unnecessary doses to surrounding normal cells during tumor treatment using a proton beam. However, if the proton beam is not irradiated at the pre-planned site, the treatment may not be effective, or most of the dose may be delivered to normal

cells near the cancer cells. The reason for the uncertainty in proton treatment is the presence of errors when determining the proton-stopping power from computed tomography (CT) images, as well as the occurrence of patient-positioning errors, errors due to patient breathing, and changes in treatment tumors owing to long-term treatment. Therefore, the organs at risk are currently considered in treatment plans, and treatment is performed with additional safety margin around the treatment site.¹⁾

To optimize proton-beam treatment, there is a need for technology that verifies the beam range²⁾ during real-time treatment. There has been focus on the prompt gamma emission that is expected to provide a more instantaneous vision of determining the beam range, because the prompt gamma distribution is similar with the proton dose distribution near the range. By measuring the prompt gamma distribution, the proton beam range determination method was confirmed for the first time using experiments by Min et al.³⁾ On the basis of these experiments, we have developed a multi-slit prompt-gamma camera that can determine the proton-beam range with a physically collimated-based verification system to measure the prompt gamma distribution.⁴⁾ In the prompt-gamma distribution acquired by this camera, there was a distribution that showed a sharp decrease in the dose falloff region; thus, a sigmoidal curve fitting-based automatic proton-beam range algorithm developed by this research team was used to determine the beam range. In addition, the multi-slit prompt-gamma camera is designed to easily expand the field-of-view (FOV). It has an advantage in that the camera can measure the prompt gamma distribution while the camera is fixed near the treatment target, irrespective of the beam energy and the irradiation location. Previous studies have confirmed that the beam range can be experimentally determined within a 2-mm error through a multi-slit gamma-camera in a homogeneous phantom. However, in a heterogeneous phantom, when the beam range is located near the boundary of two materials with a large difference in density, it was confirmed that errors increased during the determination of the beam range. This is due to the fact that the automatic proton-beam range determination algorithm cannot determine the beam range, owing to the difference

in the number of prompt gammas generated during reactions between the proton beam and materials, at the boundary surface of two materials with a large difference in densities. In this study, to improve the accuracy of proton-beam range determination in a heterogeneous phantom, we developed a method with material properties to correct the prompt-gamma distribution. To verify the performance of the developed method, we performed simulations using a multi-slit prompt-gamma camera of the prompt-gamma distribution produced by proton-beam irradiation of a combination of soft-tissue, bone, and lung-equivalent materials in four types of heterogeneous phantoms. Next, the information pertaining to the materials of the heterogeneous phantom was used to correct the acquired prompt-gamma distribution, and after correction, we used an automatic proton-beam range determination algorithm to determine the beam range. Finally, we compared the beam range that was determined by a multi-slit prompt-gamma camera and the real beam range, and we estimated the performance of the developed correction method in the heterogeneous phantom.

Materials and Methods

1. Design of the correction method

The prompt-gamma distribution, which occurs when the proton beam interacts with the heterogeneous phantom, is similar with the proton dose distribution at the distal falloff region. However, the distribution may change owing to a difference in the number of produced prompt gammas per unit volume because of differences in the density of the material and differences in the elements comprising the material. This is the reason for incorrect determination of the beam range by automatic proton-beam range determination algorithms that employ algorithms which find regions of rapid decline in prompt-gamma distributions. In this research, we developed a method to correct the difference in the number of prompt gammas.

First, the number of prompt gammas produced by a proton beam in the three types of representative materials—soft-tissue-, bone-, and lung-equivalent material—was examined using the Geant4 (version 10.03.

p01) Monte Carlo simulation tool kit. The density and element ratios of the equivalent materials were determined by referring to ICRP publication 110 and ICRU report 46, and the following values were used. For soft tissue, lung tissue, and compact bone, the density values were 1.03 g/cm³, 0.382 g/cm³, and 1.85 g/cm³, respectively^{3,6,7}. For the Monte Carlo simulations, the physics model QGSP_BERT_HP was used, and the physical behaviors of primary protons below 10 GeV and neutrons below 20 MeV were precisely simulated. Further, using the G4ParticleChange class, the prompt gammas with over 3 MeV of energy generated inside the phantom in the direction of the position of the detector were split into 10 pieces, and were assigned a weight of 0.1. In this way, the computation simulation time was decreased by irradiating the number 10 times lower than the number of actually irradiated proton beams. The computer used for the simulations had a CPU with an Intel® Xeon® Processor E5-2697 v2 with 256 GB of memory and with the CentOS7 operating system.

Based on the number of produced prompt gammas acquired from the simulation, we developed a correction equation (1), and the influence of the material properties was corrected for each measured result obtained from each detector.

$$N_{pg,c,m} = N_{pg} \times \frac{\rho_t}{\rho_m} \times \frac{\bar{s}_t}{\bar{s}_m} \times \frac{N_{total,pg,m}}{N_{total,pg,t}} \approx N_{pg} \times \frac{R_t}{R_m} \times \frac{N_{total,pg,m}}{N_{total,pg,t}} \quad <Eq. 1>$$

Equation 1 is used to obtain the corrected number of prompt gammas $N_{pg,c,m}$ considering information about the location of interest in the material. To correct the number of produced prompt gammas per unit volume, the process converted the thickness of the target material to the soft tissue-equivalent thickness,⁸⁾ and this process also involves multiplying the number of measured prompt gammas N_{pg} by the soft tissue-equivalent material to obtain the target material prompt gamma production ratio. Here, ρ_t and ρ_m refer to the densities of the soft tissue and target material, respectively. \bar{s}_t and \bar{s}_m refer to the stopping power of the soft tissue and target material, respectively. $N_{total,pg,t}$ and $N_{total,pg,m}$ refer to the number of prompt gammas produced in the soft tissue and in the target material, respectively, during proton-beam irradiation. In the correction equation, the value of the stopping power of proton and the density

was converted to the value of the range R_t and R_m for the soft tissue and target material, respectively.⁸⁾

2. Construction of heterogeneous phantom

To verify the developed method, simulations to acquire the prompt gamma distribution were performed with a multi-slit prompt-gamma camera on a phantom constructed with combined soft tissue-, lung-, and bone-equivalent material. Before evaluating a complex heterogeneous phantom with a construction similar to the human body, we performed simulations for the simple case involving the presence of bone and lung-equivalent material in soft tissue-equivalent material. An identical heterogeneous cylinder phantom with 30-cm diameter and 40-cm length was set up, and the materials were combined in the longitudinal direction. First, the heterogeneous phantom that included the bone-equivalent material was formed lengthwise in the following order: 5 cm of tissue-equivalent material, 4 cm of bone-equivalent material, and 31 cm of tissue-equivalent material (Fig. 1a). The heterogeneous phantom, which included lung-equivalent material, was constructed by substituting with lung-equivalent material only the bone-equivalent material in a heterogeneous phantom that included bone-equivalent material (Fig. 1b). Next, to simulate the conditions of a lung tumor, in the longitudinal direction, we used a heterogeneous cylindrical phantom with 5 cm of tissue-

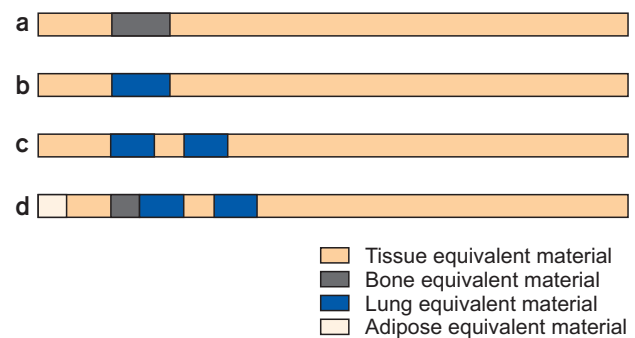


Fig. 1. Heterogeneous phantom used in Monte Carlo simulations: (a) Heterogeneous phantom with bone-equivalent material inside tissue-equivalent material, (b) heterogeneous phantom with lung-equivalent material included in tissue-equivalent material, (c) heterogeneous phantom simulating a tumor within lung-equivalent material, and (d) heterogeneous phantom constructed based on CT data of a real patient.

equivalent material, 3 cm of lung-equivalent material, 2 cm of soft tissue-equivalent material representing cancer cells, 3 cm of lung-equivalent material, and finally, 27 cm of soft tissue-equivalent material. Finally, with respect to actual patient CT data,⁹⁾ a cylindrical heterogeneous phantom was formed, which had 2 cm of adipose-equivalent material, 3 cm of tissue-equivalent material, 2 cm of bone-equivalent material, 3 cm of lung-equivalent material, 2 cm of tissue-equivalent material representing cancer cells, 3 cm of lung-equivalent material, and finally, the rest was 25 cm of soft tissue-equivalent material. For the adipose-equivalent material density and element construction, we used an adipose construction with a density of 0.95 g/cm³, as reported in ICRP publication 110. When applying this proposed method to real patients, it is expected that classification will be performed based on patients' body structure in accordance with correlations that exist between the number of CTs and the body structure.¹⁰⁾ In this study, research was performed using a multi-slit prompt-gamma camera to acquire a prompt-gamma distribution that is generated from the beam irradiation of a heterogeneous phantom of the type referred to above; information from the heterogeneous phantom material was used, and the beam range was determined after correcting the acquired prompt-gamma distribution.

3. Construction of multi-slit prompt-gamma camera

Fig. 2 shows a model that was developed using the multi-slit prompt-gamma camera employed by the Geant4 Monte Carlo simulation toolkit. The multi-slit prompt-gamma camera measures only the prompt gammas that are generated in the direction perpendicular to the beam during nuclear reactions between the proton beam and material, selectively, through the multi-slit collimator. This camera can determine the proton-beam range using the measured prompt gamma distribution. The camera is formed by two multi-slit collimators and two CsI (Tl) scintillation array-type detectors. The design was developed such that one multi-slit collimator was formed using 101 tungsten boards of size 10×10×0.2 cm³. The tungsten boards were arranged in 4-mm intervals. A total

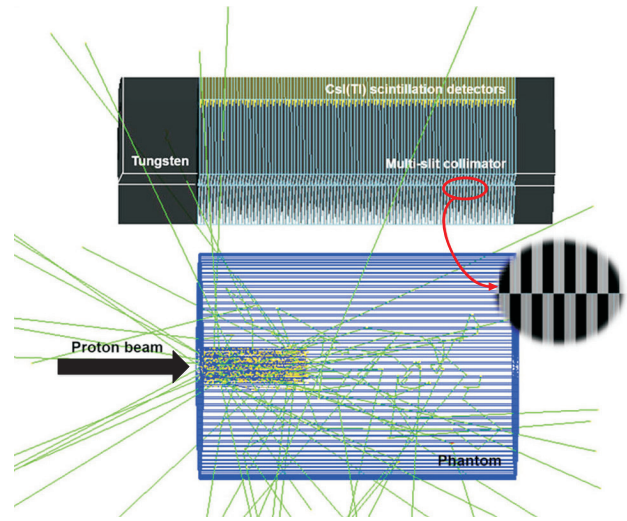


Fig. 2. Multi-slit prompt gamma-camera modeled using Geant4.

of 100 0.2×10 cm² parallel rectangular slits were arranged at 4-mm intervals. For the multi-slit collimator, at every 4-mm interval, there was a structural limitation caused by the tungsten board thickness. Therefore, the same type of multi-slit collimator was placed on another multi-slit collimator, and the slits were arranged in a crisscross pattern such that the measurement interval was 2 mm. The angle between the two multi-slit focused devices was adjusted to match the beam irradiation location. Behind each slit on the focused device, 200 thin CsI (Tl) scintillator detectors with size 10×3×0.3 cm³ were placed to acquire the prompt-gamma distribution, which has an energy that is greater than 3 MeV.

4. Correction method for prompt-gamma distribution in heterogeneous phantom

Compared to soft tissue, in the lung, the number of prompt gammas generated per unit volume is relatively low when the proton beam irradiates a heterogeneous phantom. In bones, a large number of prompt gammas are produced per unit volume. Because there is a difference in the ratio of prompt gamma production depending on the material, the number of prompt gammas obtained in a heterogeneous phantom can rapidly decrease in boundary regions between surfaces, and not in dose falloff region. Beam-range determination algorithms

that are based on the prompt-gamma distribution rely on determining the location involving a sharp decline in prompt-gamma distribution; therefore, there is the possibility of obtaining an inaccurate determination of the beam-range locations owing to the influence of the boundary surface between materials in the heterogeneous phantom. In this research, to increase the accuracy of the determined beam range in a heterogeneous phantom, the prompt-gamma distribution acquired from a multi-slit prompt-gamma camera was corrected using the material information obtained from a heterogeneous phantom. In principle, the multi-slit prompt-gamma camera measures only the prompt gamma produced in the material at the location facing the detector using the multi-slit collimator. Using this method, the prompt gammas produced with respect to the heterogeneous phantom can be corrected using only information about the inner construction of the heterogeneous phantom. The correction method is as follows:

First, the prompt gamma produced from irradiating a heterogeneous phantom with a proton beam is acquired using a multi-slit prompt-gamma camera, and the background radiation distribution is removed from the acquired prompt-gamma distribution. To remove the background radiation distribution from the prompt-gamma distribution, the slit was blocked using a tungsten board that is made of the same material as the rectangular slit of the multi-slit collimator. Then, the same proton beam is irradiated in the heterogeneous phantom, and a multi-slit prompt-gamma camera is used to acquire the distribution. Compared to the background radiation distribution when the slit is open, the acquired background radiation distribution has a similar distribution form; however, the total number of acquired rays is small. Thus, weighting is performed on the acquired distribution with a blocked slit, the actual background radiation distribution is tuned. After the smoothing method was applied, it is removed from the distribution measured in the original case when the slit was open. In this case, the weights were obtained by using the average ratio obtained by measurements when the slit is opened and closed using the three scintillation detectors at the end. In addition, for the distribution on which the background radiation influence has been removed, the

previously determined correction method is performed. Further, an additional correction is performed for the boundary surface where the two materials make contact. The additional correction is also performed based on the reference point of the boundary surface, i.e., 6 mm inside the detector. The reason for performing the additional correction is that the effect of not shielding the prompt gammas in the tungsten board of the multi-slit collimator and the influence of the scattered radiation from the surrounding detector. Finally, the existing background radiation distribution that was previously removed is then incorporated, and we obtain a distribution that is corrected for the influence of the heterogeneous phantom on the initial acquired prompt-gamma distribution.

5. Method to determine proton beam range

To determine the beam range from the corrected prompt-gamma distribution, we used a MATLAB program-based automatic proton beam-range determination algorithm⁵⁾ for the multi-slit prompt-gamma camera. The algorithm automatically sets the interval to apply the fitting around the region where the prompt gamma decreases rapidly in the obtained prompt gamma distribution, and then performs the sigmoidal curve fitting to find the inflection point. This inflection point is closely correlated to the real beam range. In this study, the value used for the beam range was the value of the inflection point obtained through sigmoidal curve fitting.

Results and Discussion

1. Variation of prompt-gamma distribution with material

To correct the prompt-gamma distribution generated in the heterogeneous phantom, the location of the prompt gamma generated from each material was obtained. Fig. 3 shows the depth locations of the produced prompt gammas when using a 150-MeV proton beam to irradiate bone-, lung-, and soft tissue-equivalent material. A proton beam of the same energy was used for irradiation, but owing to differences in the density of the material and the elements

comprising the material, it was confirmed that there was a difference in the position of the proton beam's Bragg Peak. The total numerical relative ratio of prompt gammas generated in soft tissue and materials was not influenced by the proton beam energy, and it was confirmed that only the targeted materials were influenced. The prompt gamma ratio of soft tissue to special materials that was deduced from these computer simulations was used in Equation 1.

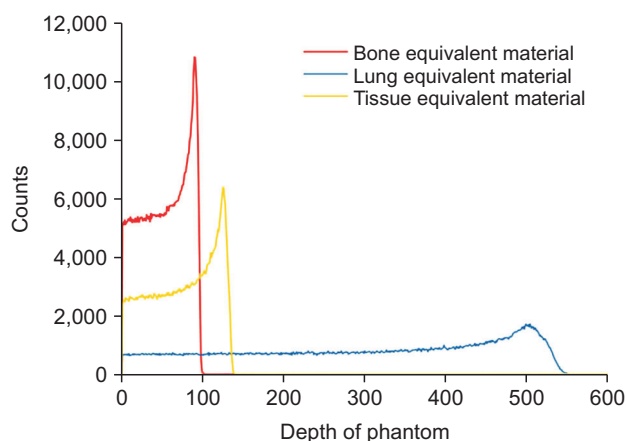


Fig. 3. Prompt gamma depth distribution generated using a 150-MeV proton beam to irradiate bone-, lung-, and tissue-equivalent materials.

2. Determination of proton beam range in heterogeneous phantom

1) Case with bone-equivalent material inside soft-tissue-equivalent material

The left side of Fig. 4 shows results of the prompt-gamma distribution, which was measured by a multi-slit prompt-gamma camera in soft-tissue-equivalent material, which included bone-equivalent material after irradiation by a proton beam from 80 MeV to 145 MeV; the proton-beam energy was varied in increments of 5 MeV. The number of proton beams used in these computer simulations was 1×10^9 . The time required for computer simulation of one case was found to be 2 h 20 min to 2 h 40 min using the server computer, and it was confirmed that there was a difference depending on the energy of the proton beam. The results showed that the number of produced prompt gammas in bone-equivalent material (black line) was higher than in the surrounding soft tissue. The right side of Fig. 4 shows the result after the influence of bone-equivalent material was corrected.

Fig. 5 shows the prompt-gamma distribution acquired in a heterogeneous phantom both before and after correction. An automatic proton-beam range algorithm was used to determine the range. A comparison of this result with the real range confirms that the ranges were determined well for both the corrected and uncorrected

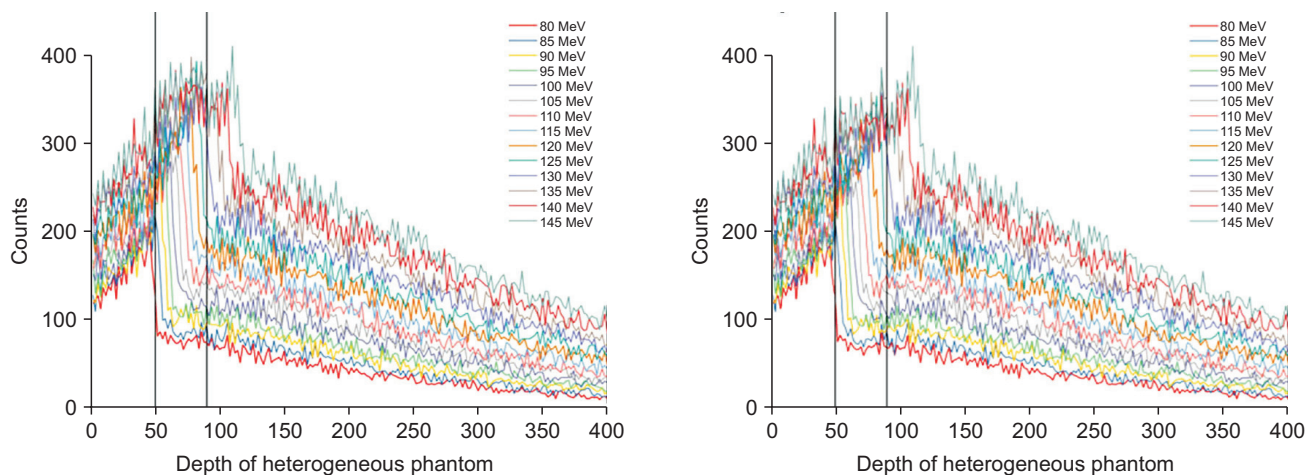


Fig. 4. Variation of prompt-gamma distribution with irradiation proton-beam energy acquired by a multi-slit prompt-gamma camera for the case with bone-equivalent material inside tissue-equivalent material (left side), and prompt-gamma distribution corrected for the influence of the heterogeneous phantom (right side).

ranges. Quantitatively, before correcting the heterogeneous phantom, the maximum difference between the calculated range and the actual range was found to be 1.8 mm using a beam-range determination algorithm. After correction, a maximum difference of 1.6 mm was demonstrated. Compared to soft tissue, the case with bone did not exhibit a large difference in the number of prompt gammas produced per unit volume, and this confirms that the beam range was determined well both before and after correction.

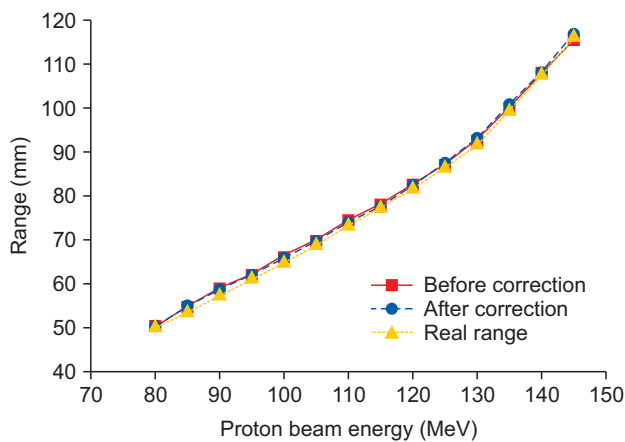


Fig. 5. Range results before and after correction of automatic proton-beam range-determination algorithms for the case with bone-equivalent material inside tissue-equivalent material.

2) Case with lung-equivalent material inside soft tissue-equivalent material

The left side of Fig. 6 shows soft tissue-equivalent material that included lung-equivalent material. The proton-beam energy was varied from 80 MeV to 125 MeV in increments of 5 MeV, and the simulation results obtained for the prompt-gamma distribution produced after irradiation, as well as those measured by multi-slit prompt-gamma camera, are shown in the figure. The number of proton beams used in the computer simulation was 1×10^9 . The density of the lung-equivalent material was 0.382 g/cm^3 , which is lower than that of the soft-tissue-equivalent material; thus, it was confirmed that the number of prompt gammas produced per unit volume was lower. In particular, in contrast to the simulation results obtained for bone-equivalent material, the difference in the prompt gamma production was comparatively high in cases with lung-equivalent material. To correct for this influence, the proposed method was used, and the results obtained for the correction of the influence of the lung-equivalent material are shown in the right side of Fig. 6.

Fig. 7 shows the range results obtained using automatic proton-beam range algorithms both before and after correction for the prompt-gamma distribution in a heterogeneous phantom. For the lung-equivalent material, at a proton-beam energy of 90 MeV, before correction, the range showed comparatively large errors compared to that

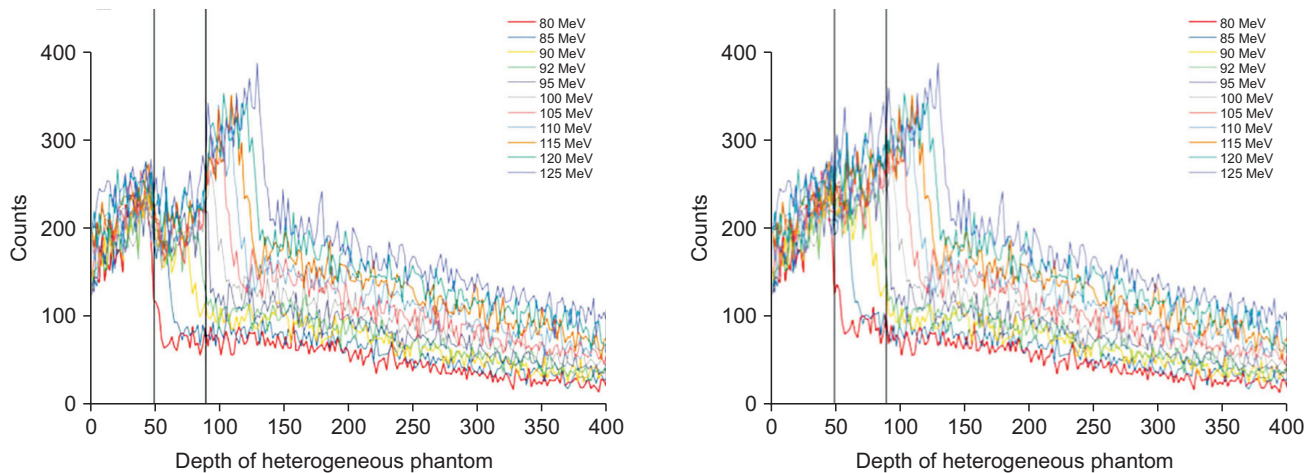


Fig. 6. Variation of prompt-gamma distribution with irradiation proton-beam energy acquired by a multi-slit prompt-gamma camera for the case with lung-equivalent material inside tissue-equivalent material (left side), and prompt-gamma distribution corrected for the influence of the heterogeneous phantom (right side).

for the real beam range. This was owing to the incorrect selection of a region in the beam-range determination algorithms. However, after correcting for the influence in the heterogeneous phantom, it was confirmed that the beam range was accurately determined. Quantitatively, before correcting for the influence in a heterogeneous phantom, using beam-range determination algorithms, the determined range exhibited a difference of approximately 18.7 mm compared with the actual value. After correction, it then showed a maximum difference of 2.2 mm. Thus, by using the proposed correction method, the beam range

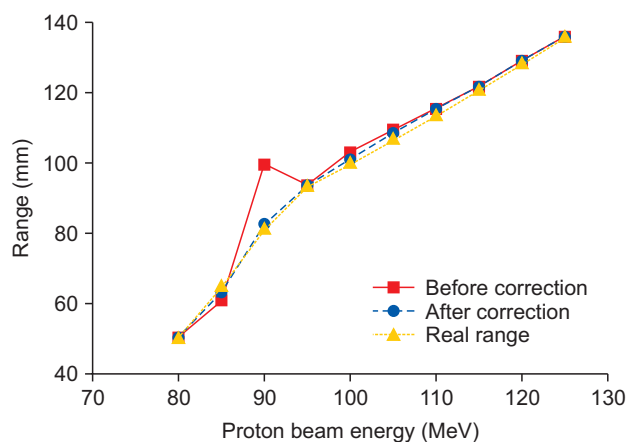


Fig. 7. Range results obtained before and after correction of automatic proton-beam range-determination algorithms for the case with lung-equivalent material inside tissue-equivalent material.

could be accurately determined, even in a low-density region such as lung.

3) Case with soft-tissue-equivalent material in between lung-equivalent material

During irradiation by a proton beam in real treatment, it is particularly difficult to determine the beam range when cancer cells exist inside the lungs as well as in low-density materials in the body. Thus, the possibility of determining the beam range was assessed even in this case. The left side of Fig. 8 shows the prompt-gamma distribution for the case of the soft-tissue that was supposed to be cancer cells, which was obtained by changing the beam energy from 80 MeV to 130 MeV in steps of 5 MeV. The number of proton beams used in this computer simulation was 1×10^9 . Similar to previous results, it was confirmed that the production of prompt gammas was low in the lung-equivalent material. The result of the correction of this influence in the heterogeneous phantom is shown in the right side of Fig. 8.

Fig. 9 shows the evaluated beam range, which was determined using automatic proton-beam determination algorithms for both corrected and uncorrected prompt-gamma distributions when there is tissue-equivalent material between lung-equivalent materials. Quantitatively, when compared with the actual range, the range determined using the beam-range determination algorithms showed a difference of 3.2 mm and 2.8 mm before and after

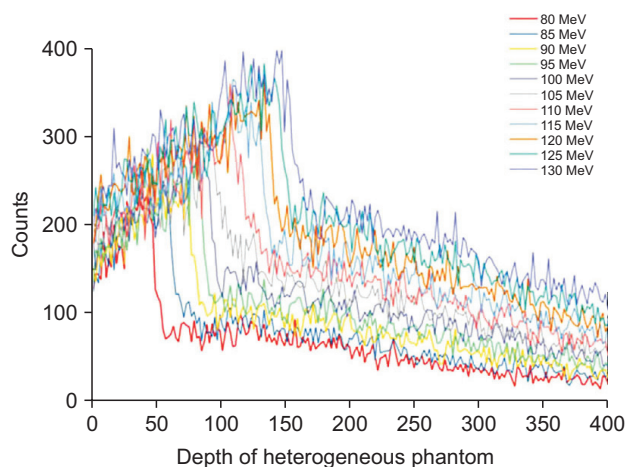
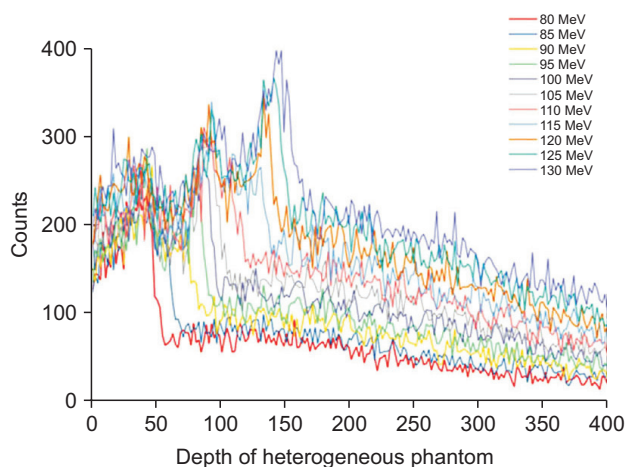


Fig. 8. Variation of prompt-gamma distribution with irradiation proton-beam energy acquired by a multi-slit prompt-gamma camera for the case with tissue-equivalent material inside lung-equivalent material (left side), and prompt-gamma distribution corrected for the influence of the heterogeneous phantom (right side).

correction, respectively. In this way, it was confirmed that even when there are tumors between lungs, the multi-slit prompt-gamma camera can be used, and a beam range with an error of approximately 3 mm can be determined.

3. Determination of proton beam range in complex heterogeneous phantom

The prompt-gamma distributions that were acquired in the heterogeneous phantom that was constructed based on the patient CT data were illustrated on the left side of Fig. 10. In this simulation, the irradiated proton-beam energy

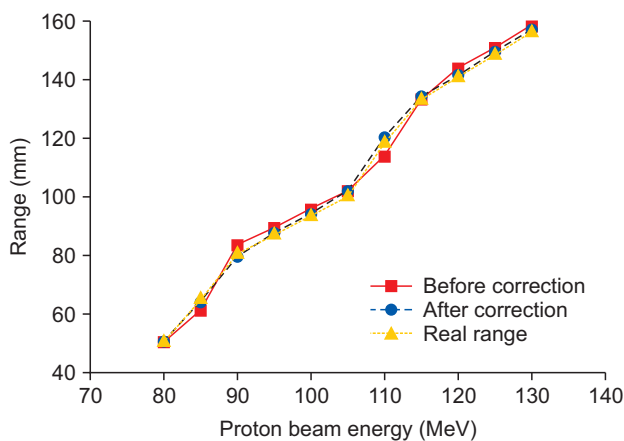


Fig. 9. Range results before and after correction of automatic proton-beam range-determination algorithms for the case with tissue-equivalent material inside lung-equivalent material.

was varied from 80 MeV to 140 MeV in increments of 5 MeV to acquire prompt-gamma distributions. To reduce the occurrence of statistical errors, for each proton-beam energy value, we used 2×10^9 protons, which was double the number of protons used in the previous simulation with the simple heterogeneous phantom. We found that such a difference of the acquired prompt gammas was significant in the region close to the boundary between the lung and the bone, as shown on the left side of Fig. 10. In contrast, the fluctuation in the prompt-gamma distribution was reduced after correcting the distribution based on material distribution data, as shown on the right side of Fig. 10.

Fig. 11 shows the beam range results for both a corrected and uncorrected complex heterogeneous phantom, which were obtained using automatic proton-beam range algorithms. The results show that in the lung-equivalent material just behind the bone-equivalent material, where the beam range was located, at a proton-beam energy of 115 MeV, a maximum error of 14.7 mm was observed in the beam-range determination; this is a large error. It is believed that this was because of the sharp decline in prompt gamma distribution, which was due to a sharp drop in the stopping power and density at the boundary surface between the two materials. In contrast, by applying the proposed correction method, the beam range can be generally found to within an error of 2.5 mm, and even in the region surrounding the boundary surface,

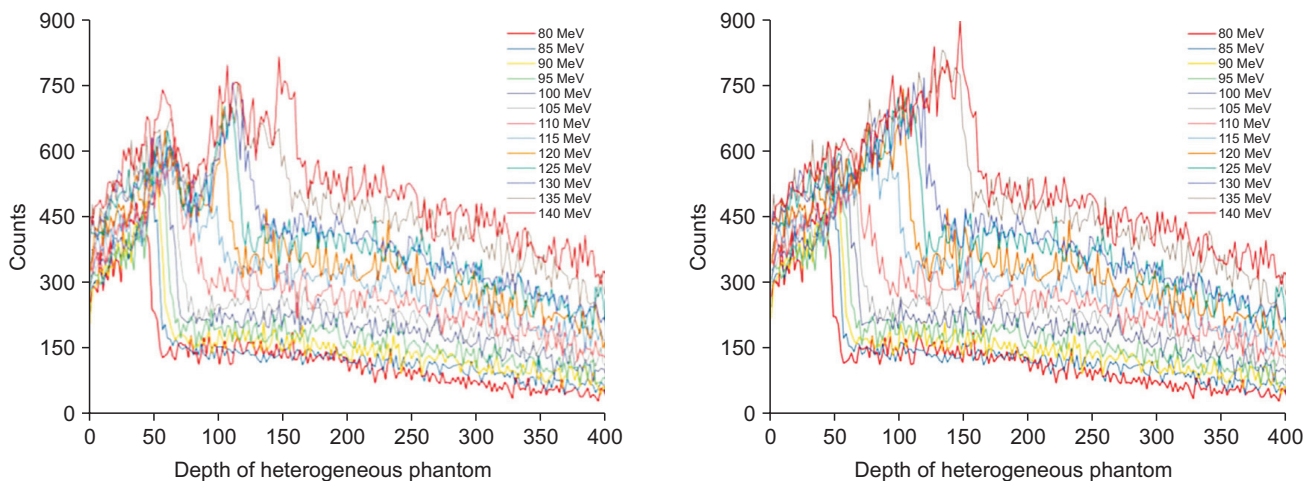


Fig. 10. Variation of prompt-gamma distribution with irradiation proton-beam energy acquired by a multi-slit prompt-gamma camera for the case of a complex heterogeneous phantom (left side), and prompt-gamma distribution corrected for the influence of the heterogeneous phantom (right side).

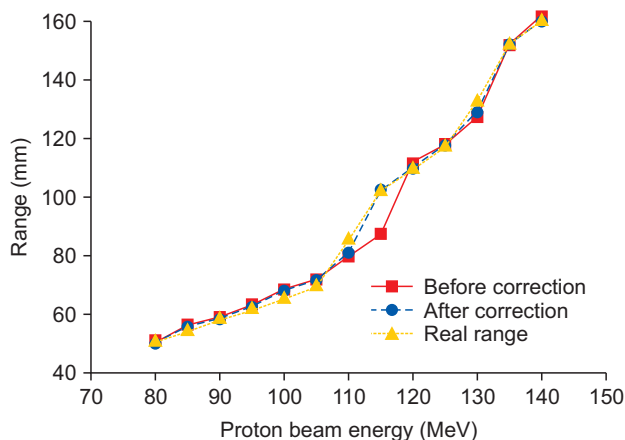


Fig. 11. Range results obtained before and after correction of automatic proton-beam range-determination algorithms for a complex heterogeneous phantom.

the maximum error is 4.1 mm, which corresponds to a comparatively accurate result. Thus, to apply the proposed correction method to a heterogeneous phantom based by CT data, it is required that the beam be delivered accurately to the location specified in the treatment plan. However, owing to reasons such as mechanical faults in the treatment devices or patient mispositioning, the beam may not be delivered to the planned beam position; in this case, if the prompt-gamma distribution is not corrected appropriately, it could cause a lower-range determination accuracy.

Before corrections, the prompt-gamma distribution measured by the camera is independently compared with the simulated prompt-gamma distribution to evaluate whether the proton beam is irradiated to the planned beam position or not. Thus, the above-mentioned problem can be solved by the above method.

Conclusion

In the present study, a method to improve the accuracy of the beam range determination in a heterogeneous phantom by correcting a prompt gamma-ray distribution was developed. The correction is based on prompt gamma emission data and beam range ratios that were acquired in advance using Monte Carlo simulations. To verify the proposed method using Monte Carlo simulation, the prompt gamma distributions were acquired by using multi-

slit prompt gamma camera for various heterogeneous phantoms and proton energies. The beam range was determined using automatic beam-range determination algorithms on the corrected prompt gamma distribution. The results showed that it was possible to confirm the beam range for the majority of the results to within 2.2 mm. In particular, in a heterogeneous phantom based on patient CT data, it was confirmed that the method can be applied appropriately, and there is good potential for the application of this approach to determine the range during actual treatment.

Verification of the method proposed in this research was performed only in the multi-slit prompt-gamma camera; however, we believe that this method can be applied to other prompt gamma measurement systems. In the future, experiments will be conducted using a therapeutic proton beam and a heterogeneous phantom. Moreover, the possibility of correcting the prompt gamma-ray distribution produced in the heterogeneous phantom, will be examined, not only in pencil beam scanning (PBS) such as single-energy proton beams, but also in spread-out Bragg peak (SOBP) beams.

Acknowledgements

This study was supported by the Electronics and Telecommunications Research Institute (ETRI) R&D Program (Development of particle beam range verification technology based on prompt gamma-ray measurements, 15ZC1810), and by the National Nuclear R&D Program through the National Research Foundation of Korea (NRF) funded by the Ministry of Education, Science, and Technology (NRF-2015M2A2A6A01045241).

Conflicts of Interest

The authors have nothing to disclose.

Availability of Data and Materials

All relevant data are within the paper and its Supporting Information files.

References

1. Paganetti H. Range uncertainties in proton therapy and the role of Monte Carlo simulations. *Phys. Med. Biol.* 2012;57:R99–R117.
2. Knopf AC, Lomax A. In vivo proton range verification: a review. *Phys. Med. Biol.* 2012;58:R131–R160.
3. Min CH, Kim CH, Youn MY, Kim JW. Prompt gamma measurements for locating the dose fall-off region in the proton therapy. *Appl. Phys. Lett.* 2006;89:183517.
4. Park JH, Lee HR, Kim SH, et al. Development of dual-mode signal processing module for multi-slit prompt-gamma camera. *Prog. Med. Phys.* 2016;27:37–45.
5. Park JH, Lee HR, Kim SH, et al. Development of automated proton beam range verification algorithm for multi-slit prompt-gamma camera. The Korean Association for Radiation Protection Autumn Meeting, Jeju, Korea; 2016.
6. ICRP publication 110. Adult reference computational phantoms; 2009:39(2).
7. ICRU Report 46. Photon, Electron, Proton and Neutron International data for Body Tissues;1992.
8. Zhang R, Newhauser W. Calculation of water equivalent thickness of materials of arbitrary density elemental composition and thickness in proton beam irradiation. *Phys. Med. Biol.* 2009;54:1383–1395.
9. Priegnitz M, Helmbrecht S, Janssens G, et al. Measurement of prompt gamma profiles in heterogeneous targets with a knife-edge slit camera during proton irradiation. *Phys. Med. Biol.* 2015;60:4849–4871.
10. Schneider W, Bortfeld T, Schlegel W. Correlation between CT numbers and tissue parameters needed for Monte Carlo simulations of clinical dose distributions. *Phys. Med. Biol.* 2000;45:459–478.